



Published in final edited form as:

Neuroimage. 2008 May 1; 40(4): 1516–1522. doi:10.1016/j.neuroimage.2008.01.043.

Neocortical Reorganization in Spina Bifida

Jenifer Juranek, Ph.D.¹, Jack M. Fletcher, Ph.D.², Khader M. Hasan, Ph.D.³, Joshua I. Breier, Ph.D.¹, Paul T. Cirino, Ph.D.^{2,4}, Paula Pazo-Alvarez, Ph.D.¹, Javier D. Diaz, Ph.D.^{5,6}, Linda Ewing-Cobbs, Ph.D.¹, Maureen Dennis, Ph.D.⁷, and Andrew C. Papanicolaou, Ph.D.¹

¹ Department of Pediatrics, University of Texas Health Science Center at Houston, Texas

² Department of Psychology, University of Houston, Houston, Texas

³ Department of Diagnostic and Interventional Imaging, University of Texas Health Science Center at Houston, Texas

⁴ Texas Institute for Measurement, Evaluation, and Statistics, University of Houston, Texas

⁵ Department of Computer Sciences, University of Houston, Texas

⁶ Centro de Estudio e Investigaciones Técnicas de Guipuzcoa, Spain

⁷ Hospital for Sick Children, Toronto, Ontario, Canada

Abstract

Normal brain development throughout childhood and adolescence is usually characterized by *decreased* cortical thickness in the frontal regions as well as region-specific patterns of *increased* white matter myelination and volume. We investigated total cerebral volumes, neocortical surface area, and neocortical thickness in 16 children with a neural tube defect, spina bifida myelomeningocele (SB), and 16 age-matched typically developing controls using a semi-automated, quantitative approach to MRI-based brain morphometry. The results revealed no significant group differences in total cerebral volume. However, group differences were observed in the global distribution of distinct tissue classes within the cerebrum: the SB group demonstrated a significant 15% reduction in total white matter and a 69% increase in cerebrospinal fluid, with no differences in total gray matter. Group comparisons of neocortical surface area assessments were significantly smaller in the occipital regions for SB, with no significant group differences in the frontal regions. Group comparisons of cortical thickness measurements demonstrated reduced cortical thickness in all regions except the frontal regions, where the SB group exhibited an *increase* relative to the PC group. Although regional patterns of thinning may be associated with the mechanical effects of hydrocephalus, the overall reduction in white matter and increased neocortical thickness in the frontal regions suggest that SB reflects a long term disruption of brain development that extends far beyond the neural tube defect in the first weeks of gestation.

Keywords

Spina bifida; aMRI; cortical thickness; hydrocephalus; brain plasticity

Corresponding Author: Jenifer Juranek, Ph.D., Department of Pediatrics, Children's Learning Institute, University of Texas Medical School, 7000 Fannin, Ste 2401, Houston TX 77030, 713.500.3888 (Voice), 713.500.3878 (fax), Email: Jenifer.Juranek@uth.tmc.edu.

Publisher's Disclaimer: This is a PDF file of an unedited manuscript that has been accepted for publication. As a service to our customers we are providing this early version of the manuscript. The manuscript will undergo copyediting, typesetting, and review of the resulting proof before it is published in its final citable form. Please note that during the production process errors may be discovered which could affect the content, and all legal disclaimers that apply to the journal pertain.

Introduction

Normal brain development is characterized by a complex set of age-related transitions that involve regional calibration of the relative thickness of gray and white matter. Converging lines of evidence from histological (Yakovlev and Lecours, 1967) and neuroimaging studies (reviewed by Paus et al., 2001) indicate that white matter increases in overall volume with increased myelination occurring in a region-specific manner throughout childhood and adolescence. Specifically, spatially- and temporally-specific patterns of changes in gray matter density relative to white matter density occur earlier in parietal regions than frontal regions, while temporal regions mature later than other cortical regions (Giedd et al., 1999; Gogtay et al., 2004; Gogtay et al., 2002; Sowell et al., 2003). In a recent report (O'Donnell et al., 2005), cortical thickness of the frontopolar area was described in typically developing children and adolescents. Specifically, a linear *decrease* in cortical thickness of the frontopolar regions was observed as a function of age that was not influenced by gender or hemispheric interactions. Thus, generalized patterns of posterior to anterior gradient changes in gray and white matter densities as a function of chronological age have been previously described as part of normal development.

Studies of abnormal brain development have largely focused on losses in the brain (e.g. volume, cortical thickness, and myelin). However, abnormal brain development could involve more complex patterns of reorganization in which some brain regions are smaller than expected, while others are larger than expected. Spina bifida (SB) is a congenital disorder that affects the spine and brain when the spinal lesion is a myelomeningocele (Reigel and Rotenstein, 1994). At the level of the brain, a characteristic malformation of the cerebellum and hindbrain (Chiari II malformation) obstructs the flow of cerebrospinal fluid (CSF) and leads to significant hydrocephalus in children born with SB and the open spinal lesion known as a myelomeningocele. Furthermore, due to the decreased size of the posterior fossa (Salman et al., 2006), children with SB often have midbrain anomalies (e.g., beaking of the tectum). Finally, many with SB have a congenital partial absence of the corpus callosum that affects the rostrum, posterior body and splenium, or both (Barkovich, 2005).

In terms of neurobehavioral outcomes, relatively few children with SB sustain severe mental retardation; in fact, many have specific cognitive strengths as well as weaknesses (Fletcher et al., 2005). These strengths include word recognition, vocabulary and grammar, facial recognition, persistence of attention and effort, and certain social skills. Weaknesses involve reading and language comprehension, spatial construction skills, attention orientation and engagement, and behavioral regulation.

Less clear are the neural correlates of these outcomes. There are only a few quantitative studies of anomalous structural development of the brain in SB (Dennis et al., 2005; Dennis et al., 2006; Fletcher et al., 1996). Most of these studies were volumetric and implemented semi-automated methodologies to segment the brain. Major findings of these previous studies included significantly smaller cerebellar volumes and area measurements of the corpus callosum in SB compared to age-matched controls. In contrast, differences in total volume of the cerebrum were not apparent. Rather, reductions in gray and white matter, with a corresponding increase in CSF were restricted to large regions of the brain posterior to the genu of the corpus callosum; no differences were found in regional subdivisions anterior to the genu (Fletcher et al., 2005). However, these studies did not involve specific anatomically-defined brain regions; only *en bloc* regional definitions were available to subdivide the cerebrum into pre-, peri-, and retro-callosal regions with superior and inferior aspects of each (Filipek et al., 1994).

The present study is concerned with neocortical volume, cortical thickness, and surface area measurements in children with SB. Even more importantly, this study seeks answers to questions regarding anatomically defined regional patterns of thickening or thinning, and their implications for reorganization of the brain after multiple structural malformations and hydrocephalus associated with SB.

Hydrocephalus in SB results from an obstruction produced by the Chiari II malformation, which blocks the flow of CSF at the level of the fourth ventricle (Reigel and Rotenstein, 1994). Internal hydrocephalus occurs in which the subarachnoid spaces are filled with CSF, leading to ventricular dilation that distends the brain, stretching axons and killing cells (Del Bigio, 2004). Since the CSF flow proceeds from the site of the obstruction in the posterior brain forward into anterior regions, hydrocephalus may underlie thinning of the cortical mantle maximally in more posterior temporal, parietal, and occipital regions (Del Bigio, 2004; Raimondi, 1994). Such reports would be consistent with older studies based on pneumoencephalography and cerebral tomography that visualized a thinner cortical mantle in SB, especially in more posterior regions in some children (Dennis et al., 1981; Tromp et al., 1979). A recent study also suggests selective thinning of the cortical mantle based on visualization and measurement of individual MRI scans (Miller et al., in press). As Miller et al. noted, these observations have not been supported by information from quantitative measures.

We used contemporary neuroimaging and quantitative methods to determine whether group differences are evident in the spatial patterns of cortical thickening or thinning in SB. We hypothesized that, relative to controls, cortical thickness would be comparable in the frontal regions and thinner in the parietal and occipital regions, reflecting a developmental reorganization of the SB brain. In addition, we hypothesized that measures of the surface area of the neocortex would be smaller in more posterior regions, reflecting shrinkage of the cerebral white matter.

Materials and methods

Participants

As part of two ongoing studies, 16 children with SB and 16 age-matched pediatric controls completed the same MRI protocol lasting less than 45 minutes. Children with SB were born with myelomeningocele (verified by medical record review of pathology and neurosurgical operative reports) and shunted for hydrocephalus. All participants with SB had the characteristic Chiari II malformation and had been shunted on the right side.

The controls were recruited as typically-developing volunteers through advertisements as part of a separate study examining recovery from traumatic brain injury, but received the same imaging sequence at the same imaging center. Since we did not expect gender or ethnicity to contribute as much as age to variability across participants, group selection focused on matching children with SB and controls within 4 months of age. Children with SB averaged 12.4 (SD = 2.9) years of age at time of imaging (range of 8.75 – 17.1 years); those selected as controls averaged 12.3 (SD = 3.0) years of age (range 7.9 – 16.7 years). The SB and control groups did not significantly differ on age of MRI scan, $t(29.96) = 0.19$; $p > 0.92$. Gender ratios (M: F) were 9:7 for the group with SB and 6:10 for the controls. Based on a handedness survey, 13 participants with SB were right-handed (8 male and 5 female), while 14 controls were right-handed (4 male and 10 female). Participants with SB received the four subtest form of the Stanford-Binet Intelligence test, 4th Edition (Thorndike et al., 1986), from which a composite was generated. Controls received the two-subtest version of the Wechsler Abbreviated Scales of Intelligence (Wechsler, 1999). Given the use of different measures, we did not compare

these participants directly, although as expected, participants with SB had lower IQ scores (Mean = 80.4, SD = 14.7) than controls (Mean = 111.8, SD = 14.9).

All children were primarily English-speaking and medically stable at the time of the assessments. Written informed consent was obtained from the guardians and adolescents and assent from the children participating in these studies per the University of Texas Health Science Center at Houston and University of Houston regulations for the protection of human research subjects.

MRI Acquisition

High resolution brain MR images were acquired on a Philips 3T scanner with SENSE (Sensitivity Encoding) technology. After conventional sagittal scout and coronal T2-weighted sequences, a three-dimensional T1-weighted sequence was performed to obtain whole brain coverage. Acquisition parameters of the 3D turbo fast spin echo sequence were as follows: repetition time/echo time = 6.5–6.7/3.04–3.14; flip angle = 8 degrees; field of view=192×192mm; matrix=256×256mm; slice thickness=1.5mm; in-plane pixel dimensions (x, y) =0.94, 0.94mm; number of excitations (NEX) =2.

MRI Processing

Individual scan preparation—All scans were analyzed blind to diagnosis, age, and gender. T1-weighted images were reviewed for image quality prior to performing morphometric analyses. Using Freesurfer v3.0.4 software (www.surfer.nmr.mgh.harvard.edu) on a 64-bit Linux computer, a fully-automated process was used to skull-strip and segment each brain into 3 classes of voxels: gray matter, white matter, and CSF (Dale and Sereno, 1993; Dale et al., 1999).

Results of each of the automatic segmentations were visually inspected for accuracy using Freesurfer's Tkmedit viewer. Subsequently, within Freesurfer, a fully automated cortical reconstruction procedure was executed for producing a detailed geometric description (e.g. regular tessellation of the cortical surface consisting of ~150,000 equilateral triangles known as vertices in each hemisphere) of the CSF/GM/WM boundaries of the neocortical mantle. Cortical thickness values were automatically quantified within Freesurfer on a vertex-by-vertex basis by computing the average shortest distance between the white matter boundary and the pial surface (Fischl and Dale, 2000).

Within each hemisphere, 32 cortical parcellation units of the neocortex were automatically identified and labeled according to the Desikan atlas of gyral-based definitions included within Freesurfer's automatic cortical parcellation routine (Desikan et al., 2006). A total of three morphometric variables were investigated in each parcellation unit: cortical thickness, neocortical volume, and surface area. Each of the three morphometric variables was averaged across all vertices within each parcellation unit for each subject, yielding three separate matrices of 32 average measurements per hemisphere per subject per morphometric variable. For regional analyses, cortical parcellation units were aggregated into one of the following regions in each hemisphere: frontal, parietal, temporal, occipital, or cingulate.

Surface-based visualization of group analyses—To depict between group differences in cortical thickness measurements, an average subject was generated within Freesurfer by inflating, registering, and morphing all 32 individual brains into an average spherical surface representation (Fischl et al., 1999a; Fischl et al., 1999b). The average subject created from all participants in the study served as the target image, or common space, for displaying the results of group-level analyses. Subsequently, surface smoothing was performed using a full-width/half-maximum Gaussian kernel of 10mm.

Freesurfer's `mri_glmfit` command was executed to fit a general linear model at each vertex in the cortical mantle to perform between group averaging and statistical inference on the cortical surface. This process models the data as a linear combination of effects explained by variables of interest, confounds, and errors. The design matrix specified each class to have its own offset but all classes were forced to have the same slope (doss; different onset, same slope). The specified contrast vector (e.g. $[-1, 1, 0]$) tested for significant group differences without any regressors. In order to correct for multiple comparisons, a full Monte Carlo Simulation within Freesurfer was utilized to simulate white Gaussian noise data under the null hypothesis, with the results smoothed, and repeated for 10,000 iterations.

Statistical Analyses

Global volumetrics defined as total brain volume of the cerebrum, excluding the cerebellum, were evaluated for group differences in the distribution of tissue type within the cerebrum (e.g. gray matter, white matter, and CSF) with ANOVA where tissue type was the within subject variable and group membership was the between subject variable. Group effects on neocortical thickness, volume, and surface area were evaluated independently using a multivariate approach to a mixed model design with Region of Interest (ROI; Frontal, Parietal, Temporal, Occipital, Cingulate) and hemisphere (Left, Right) as within subject variables and Group (PC, SB) as the between subject variable. Initial analyses indicated no main effects or interactions involving hemisphere, so left and right ROIs were collapsed across hemispheres. Only significant effects (overall $\alpha < 0.05$) involving group differences are reported. Bonferroni correction was used for multiple comparisons.

Results

Global volumetrics

To ensure that group differences in regional measures did not reflect group differences in brain size, an initial analysis compared groups in total cerebrum size. The cerebellum was deliberately excluded from this analysis since previous studies have clearly demonstrated significant reductions in cerebellar volume in SB (Fletcher et al., 2005). No significant group differences in total cerebral brain volume were observed [Mean, SD: SB = $1,077\text{cm}^3$, $\pm 120.2\text{cm}^3$; PC = $1,144\text{cm}^3$, $\pm 99.9\text{cm}^3$, $t(29.03) = -1.71$, $p > 0.09$]. These results are consistent with published reports of global volumetric analyses in much larger samples of SB (Fletcher et al., 1996; Fletcher et al., 2005).

As shown in Figure 1, volumetric analyses of three-class segmentation of the cerebrum (cortical and subcortical) into gray matter, white matter, or CSF yielded a significant tissue-class by group effect, $F(2,29) = 6.64$, $p < 0.005$. Follow-up analyses evaluated group effects within tissue-class using a critical level of alpha of $p < 0.016$ ($.05/3$). There were significant group differences in white matter volumes, $F(1, 30) = 10.11$, $p = 0.0034$. However, no significant differences in gray matter volumes were apparent, as values for the two groups were within 1% of each other, $F(1, 30) = 0.09$, $p = 0.77$. The evaluation of CSF differences showed increased CSF in SB, but did not meet the critical threshold of alpha, $F(1, 30) = 6.21$, $p = 0.0184$. While the average CSF volume was *increased* by 69% and was more variable in the SB group, the average white matter volume was *decreased* by 15% in the SB group relative to the control group. Group comparisons of gray: white matter ratios demonstrated that the SB group had a significantly higher ratio (1.77) than the PC group (1.51), highlighting group differences, $F(1, 30) = 10.26$, $p < 0.004$, in white matter volumes (SB < PC) in the presence of similar gray matter volumes.

Regional Comparisons of Neocortical Morphometrics

Mean and standard deviations for volume, surface area, and thickness for each of the neocortical ROIs (cingulate, frontal, temporal, parietal, and occipital regions) are reported in Table 1 for each of the two groups (SB and controls). For volume there was a significant ROI by Group interaction, $F(4, 27) = 10.03$, $p < .0001$. Follow-up analyses evaluated group effects within each ROI collapsed across hemispheres, which did not generate significant interactions or main effects, using a critical alpha level of $p < .01$ for each ROI (.05/5). There were significant group effects showing smaller volumes in the group with SB for all ROIs except frontal: temporal, $F(1, 30) = 8.19$, $p < .008$, parietal, $F(1, 30) = 9.31$, $p < .005$, cingulate, $F(1, 30) = 7.49$, $p < 0.01$, and occipital, $F(1, 30) = 4.15$, $p < 0.05$. The mean neocortical volume for the five ROIs is plotted by group in Figure 2, showing that cortical volumes in the five ROIs tended to be greater in the controls as compared to the group with SB in all of the ROIs *except* for the frontal region, where the SB group was comparable in volume relative to the PC group.

For surface area, there was a significant ROI by group interaction, $F(4, 27) = 4.35$, $p < 0.008$. Follow up analyses evaluated the effects of group within ROI collapsed across hemispheres (given the absence of an interaction with hemisphere) using a critical value of $p < 0.01$ (0.05/5). The only significant group effect involved the occipital region, $F(1, 30) = 11.01$, $p < 0.003$. Surface area in each of the five ROIs is plotted as a function of group in Figure 3, showing a trend for surface area to be generally decreased in the SB group relative to the PC group in each of the ROIs, including the frontal region, where cortical thickness values are comparable between groups.

For cortical thickness, there was again a significant ROI by group interaction, $F(4, 27) = 23.75$, $p < 0.0001$, with no significant interactions or main effects involving hemisphere. Follow up analyses evaluated the effects of group within ROI collapsed across hemispheres using a critical value of $p < 0.01$ (0.05/5). The only significant effect of group was for the frontal region, $F(1, 30) = 16.32$, $p < 0.0003$. Cortical thickness across ROIs are plotted as a function of group in Figure 4, showing that the group with SB demonstrated *increased* cortical thickness relative to the controls in the frontal region. Example single-subject cortical thickness maps are depicted in Figure 5 for a PC and an SB subject.

Figure 6 provides the results of vertex-by-vertex group comparisons displayed on the study-specific average brain generated within Freesurfer using all 32 subjects. Significant group differences in cortical thickness are depicted based on clusters corrected for multiple comparisons using a full Monte Carlo simulation (as described in the methods section). The frontal region is unique for large clusters of increased cortical thickness in the group with SB. In contrast, parietal, occipital and temporal regions are characterized by focal clusters of decreased cortical thickness in the group with SB.

Discussion

These findings suggest substantial structural reorganization of the brain in children with SB relative to typically-developing age-matched controls. Whereas O'Donnell et al. (2005) and others (Sowell et al., 2007) reported *decreased* frontal cortical thickness in normal development as well as in children and adults with ADHD (Makris et al., 2007; Shaw et al., 2006), an opposite pattern of *increased* frontal cortical thickness was observed in the group with SB, independent of age. Furthermore, group comparisons of surface area demonstrated a significant reduction in SB, especially in the occipital lobe, which may be directly related to the global reduction in cerebral white matter observed in the group with SB. The findings do not reflect differences in the size of the cerebrum, which did not significantly differ between controls and the group with SB. Thus, while decreased surface area and neocortical volume tend to follow an anterior to posterior gradient of increasing group differences and increased variability within the SB

group, neocortical volume in the frontal region is similar between both groups. This finding is consistent with published studies of animal models of hydrocephalus and post mortem studies of humans with hydrocephalus where destruction of periventricular white matter was associated with increased ventricular size and the frontal region was predominately spared (Del Bigio et al., 2003).

Although the posterior to anterior gradient of thinning is consistent with the mechanical effects of hydrocephalus on the brain (Del Bigio, 2004), hydrocephalus does not explain why cortical thickness is *increased* in frontal regions for children with SB. Since decreased cortical thickness has been reliably associated with increased age, it is not likely that this finding is an artifact of the morphometric methods. Moreover, a recent diffusion tensor imaging study of anisotropy in association pathways (Hasan et al., in press) reported an absence or reversed pattern of age-related changes in SB relative to controls. Therefore, one possible explanation is that the increased cortical thickness is compensatory and develops in a manner that mediates areas of preserved function in SB. Since cognitive skills involving language, word recognition, and inhibitory control are mediated by neural networks that involve the frontal regions, the preservation of these skills in many with SB may reflect more reliance on the frontal components of these networks. Evidence from recently published studies in ADHD adults and children, populations characterized by poor inhibitory control, are consistent with this hypothesis as the authors reported decreased cortical thickness in the frontal-striatal regions (Makris et al., 2007; Shaw et al., 2006).

There are other indications that the disruption of brain development and reorganization in SB extends beyond the effects of hydrocephalus and the Chiari II malformation. In addition to a high frequency of stenogyria and gray matter heterotopias (Gilbert et al., 1986; Miller et al., in press), it is well known that many children with SB show abnormalities of the corpus callosum that reflect hypogenesis of the rostrum and posterior body and splenium (Barkovich 2005; Miller et al., in press). Since the corpus callosum is usually thinned by chronic hydrocephalus, these abnormalities imply that the reduction in white matter observed in this study reflect a more general disruption of white matter development that is exacerbated by hydrocephalus, with regional differences in white matter distribution reflecting the mechanical effects of hydrocephalus that will vary across individual children. Such findings are consistent with diffusion tensor imaging studies of SB, which find reduced anisotropy in several white matter structures (e.g. corpus callosum, arcuate fasciculus) and in different association fibers suggestive of reduced myelination (Hasan et al., in press; Hasan et al., 2006). However, in the caudate nucleus, transverse diffusivity is decreased and functional anisotropy is increased, which may be due to a delay in synaptogenesis. These additional findings show that other imaging modalities also find increases and decreases in different quantitative indices of brain integrity in SB.

An important implication of this study is that the early disruption of brain development that begins *in utero* in children with SB and that produces the stigmata of the Chiari II malformation is followed by a second wave of disrupted brain development that causes both hypoplasia (likely from hydrocephalus) and aberrant, regionally-specific configurations of gray and white matter. Although purely volumetric studies of gray matter *in vivo* have failed to capture the dynamic relation among volume, cortical thickness, and surface area in the neocortex of the human brain, recent advances in neuroimaging acquisition and analysis converge in demonstrating this relation. The regional specificity of our findings (e.g., greatest group differences observed in the posterior regions and comparable or trend reversal in the frontal regions) suggests that cognitive strengths and weaknesses in the SB population may be related to these regional patterns of reorganization. What is not known is whether the pattern of increased cortical thickness is adaptive or related to an aberrant pattern of brain development.

To evaluate this possibility, a larger sample is needed to determine if inter-subject variability in morphometric variables is predictive of cognitive performance in a domain-specific fashion.

Acknowledgements

This work is funded by NIH-NICHD grants, P01-HD35946 awarded to JMF and grant NICHD-R01-NS046308 awarded to LEC. Additional funding to KMH is provided by NINDS R01-NS052505. We wish to thank Vipul Kumar Patel for assistance with MRI data acquisition and Amy Walker Hampson for recruitment of spina bifida participants.

References

- Barkovich, J. Pediatric neuroimaging. 4. Lippincott, Williams & Wilkens; Philadelphia, PA: 2005.
- Dale A, Sereno MI. Improved Localization of cortical activity by combining EEG and MEG with MRI cortical surface reconstruction: A linear approach. *Journal of Cognitive Neuroscience* 1993;5:162–176.
- Dale AM, Fischl B, Sereno MI. Cortical Surface-Based Analysis: I. Segmentation and Surface Reconstruction. *NeuroImage* 1999;9:179–194. [PubMed: 9931268]
- Del Bigio M. Cellular damage and prevention in childhood hydrocephalus. *Brain Pathology* 2004;14:317–324. [PubMed: 15446588]
- Del Bigio M, Wilson M, Enno T. Chronic Hydrocephalus in Rats and Humans: White matter Loss and Behavior Changes. *Annals of Neurology* 2003;53:337–346. [PubMed: 12601701]
- Dennis M, Edelman K, Frederick J, Copeland K, Francis D, Blaser S, Kramer L, Drake J, Brandt M, Hetherington R, Fletcher J. Peripersonal spatial attention in children with spina bifida: associations between horizontal line bisection and congenital malformations of the corpus callosum, midbrain, and posterior cortex. *Neuropsychologia* 2005;43:2000–2010. [PubMed: 15893777]
- Dennis M, Fitz C, Netley C, Sugar J, Harwood-Nash D, Hendrick E, Hoffman H, Humphreys R. The intelligence of hydrocephalic children. *Archives of Neurology* 1981;38:607–615. [PubMed: 6975094]
- Dennis M, Jewell D, Edelman K, Brandt M, Hetherington R, Blaser S, Fletcher J. Motor learning in children with spina bifida: intact learning and performance on a ballistic task. *Journal of International Neuropsychological Society* 2006;12:598–608.
- Desikan RS, Segonne F, Fischl B, Quinn BT, Dickerson BC, Blacker D, Buckner RL, Dale AM, Maguire RP, Hyman BT, Albert MS, Killiany RJ. An automated labeling system for subdividing the human cerebral cortex on MRI scans into gyral based regions of interest. *NeuroImage* 2006;31:968–980. [PubMed: 16530430]
- Filipek PA, Richelme C, Kennedy DN, Caviness VS. The young adult human brain: An MRI-based morphometric analysis. *Cerebral Cortex* 1994;4:344–360. [PubMed: 7950308]
- Fischl B, Dale A. Measuring the thickness of the human cerebral cortex from magnetic resonance images. *Proceedings of the National Academy of Science, USA* 2000;97:11050–11055.
- Fischl B, Sereno MI, Dale AM. Cortical Surface-Based Analysis: II: Inflation, Flattening, and a Surface-Based Coordinate System. *NeuroImage* 1999a;9:195–207. [PubMed: 9931269]
- Fischl B, Sereno MI, Tootell R, Dale A. High-resolution intersubject averaging and a coordinate system for the cortical surface. *Human Brain Mapping* 1999b;8:272–284. [PubMed: 10619420]
- Fletcher J, Brookshire B, Landry S, Bohan T, Davidson K, Francis D, Levin H, Brandt M, Kramer L, Morris R. Attentional skills and executive functions in children with early hydrocephalus. *Developmental Neuropsychology* 1996;12:53–76.
- Fletcher JM, Copeland K, Frederick J, Blaser S, Kramer L, Northrup H, Hannay H, Brandt M, Francis D, Villarreal G, Drake J, Laurent J, Townsend I, Inwood S, Boudousquie A, Dennis M. Spinal lesion level in spina bifida: a source of neural and cognitive heterogeneity. *Journal of Neurosurgery* 2005;102:268–279. [PubMed: 15881750]
- Giedd JN, Blumenthal J, Jeffries NO, Castellanos FX, Liu H, Zijdenbos A, Paus T, Evans AC, Rapoport J. Brain development during childhood and adolescence: A longitudinal MRI study. *Nature Neuroscience* 1999;2:861–863.
- Gilbert J, Jones K, Rorke L, Chemoff G, James H. Central nervous system anomalies associated with meningocele, hydrocephalus, and the Arnold-Chiari malformation: reappraisal of theories

regarding the pathogenesis of posterior neural tube closure defects. *Neurosurgery* 1986;18:559–564. [PubMed: 3714003]

Gogtay N, Giedd J, Lusk L, Hayashi K, Greenstein D, Vaituzis A, Nugent T, Herman D, Clasen L, Toga A, Rapoport J, Thompson P. Dynamic mapping of human cortical development during childhood through early adulthood. *Proceedings of the National Academy of Science, USA* 2004;101:8174–8179.

Gogtay N, Giedd J, Rapoport JL. Brain development in healthy, hyperactive, and psychotic children. *Arch Neurol* 2002;59:1244–1248. [PubMed: 12164719]

Hasan K, Eluvathingal T, Kramer LA, Ewing-Cobbs L, Dennis M, Fletcher JM. White matter structural abnormalities in children with spina bifida myelomeningocele and hydrocephalus: A diffusion tensor tractography study of the association pathways. *Journal of Magnetic Resonance Imaging*. in press
 Hasan, K.; Sankar, A.; Kramer, LA.; Ewing-Cobbs, L.; Brandt, ME.; Hannay, HJ.; Blaser, S.; Dennis, M.; Fletcher, JM. Diffusion Tensor Imaging of the Spina Bifida Myelomeningocele at 3.0T: Preliminary evidence of neurodevelopmental brain plasticity. *International Society of Magnetic Resonance in Medicine*; Seattle, Washington: 2006.

Makris N, Biederman J, Valera E, Bush G, Kaiser J, Kennedy D, Caviness V, Faraone S, Seidman L. Cortical thinning in the attention and executive function networks in adults with attention-deficit/hyperactivity disorder. *Cerebral Cortex* 2007;17:1364–1375. [PubMed: 16920883]

Miller E, Widjaja E, Blaser S, Dennis M, Raybaud C. The old and the new: Supratentorial MR findings in Chiari II malformation. *Child's Nervous System*. in press

O'Donnell S, Noseworthy MD, Levine B, Dennis M. Cortical thickness of the frontopolar area in typically developing children and adolescents. *NeuroImage* 2005;24:948–954. [PubMed: 15670671]

Paus T, Collins D, Evans A, Leonard G, Pike B, Zijdenbos A. Maturation of white matter in the human brain: a review of magnetic resonance studies. *Brain Research Bulletin* 2001;54:255–266. [PubMed: 11287130]

Raimondi A. A unifying theory for the definition and classification of hydrocephalus. *Child's Nervous System* 1994;10:2–12.

Reigel, D.; Rotenstein, D. Spina bifida. In: Cheek, W., editor. *Pediatric neurosurgery*. WB Saunders; Philadelphia: 1994. p. 51-76.

Salman M, Blaser S, Sharpe J, Dennis M. Cerebellar vermis morphology in children with spina bifida and Chiari type II malformation. *Child's Nervous System* 2006;22:385–393.

Shaw P, Lerch J, Greenstein D, Sharp W, Clasen L, Evans A, Giedd J, Castellanos F, Rapoport J. Longitudinal mapping of cortical thickness and clinical outcomes in children and adolescents with attention-deficit/hyperactivity disorder. *Archives of General Psychiatry* 2006;63:540–549. [PubMed: 16651511]

Sowell E, Peterson B, Kan E, Woods R, Yoshii J, Bansal R, Xu D, Zhu H, Thompson P, Toga A. Sex differences in cortical thickness mapped in 176 healthy individuals between 7 and 87 years of age. *Cerebral Cortex* 2007;17:1550–1560. [PubMed: 16945978]

Sowell ER, Peterson BS, Thompson PM, Welcome SE, Henkenius AL, Toga AW. Mapping cortical change across the human life span 2003;6:309–315.

Thorndike, R.; Hagen, E.; Sattler, J. *The Stanford-Binet Intelligence Scale*. 4. Riverside; Itasca, IL: 1986.

Tromp C, van den Burg J, de Vries S. Nature and severity of hydrocephalus and its relation to later intellectual function. *Zeitschrift fur Kinderchirurgie* 1979;28:354–360.

Weschler, D. *Weschler abbreviated scales of intelligence*. Psychological Corp; New York: 1999.

Yakovlev, P.; Lecours, A. The Myelogenetic Cycles of Regional Maturation of the Brain. In: Minkowski, A., editor. *Regional Development of the Brain in Early Life*. Blackwell Scientific Publications; Paris, France: 1967. p. 3-70.

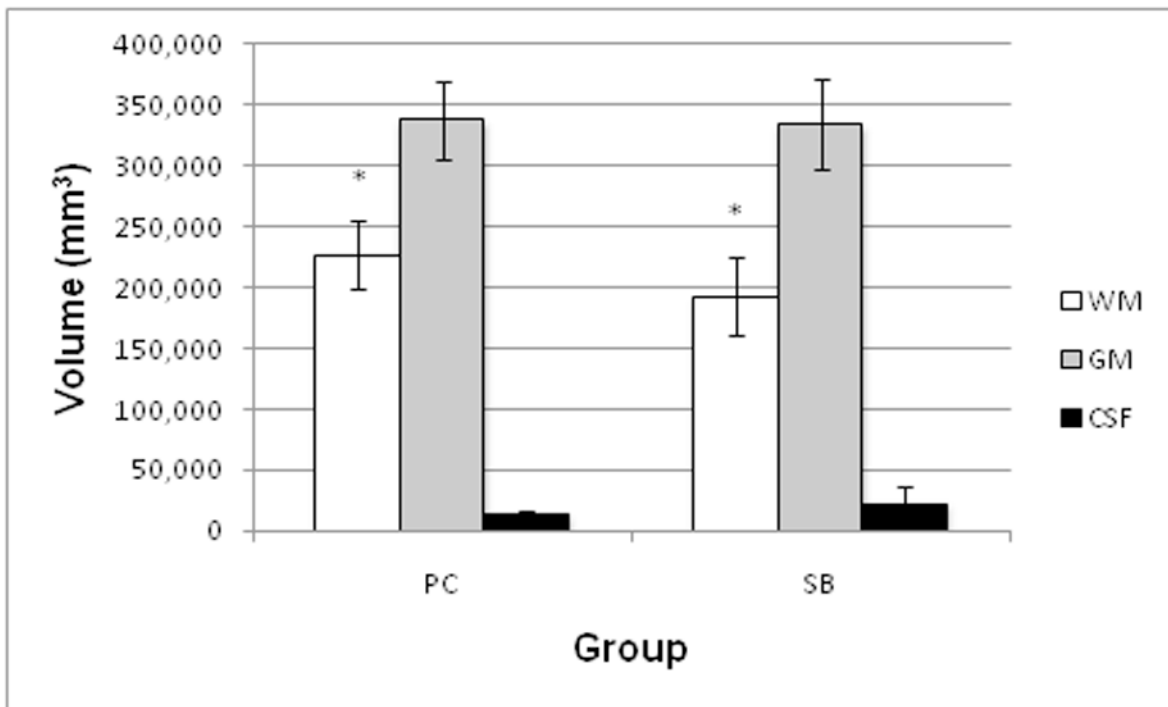


Figure 1. Group comparisons of three-class segmentation volumetrics of the cerebrum (e.g. cerebellum is not included): White Matter (WM), Gray Matter (GM), Cerebrospinal fluid (CSF) White matter volume is significantly reduced in SB relative to PC (*); CSF volume is increased in SB relative to SB; GM is comparable in both groups. Values shown are Mean +/- SD (mm³).

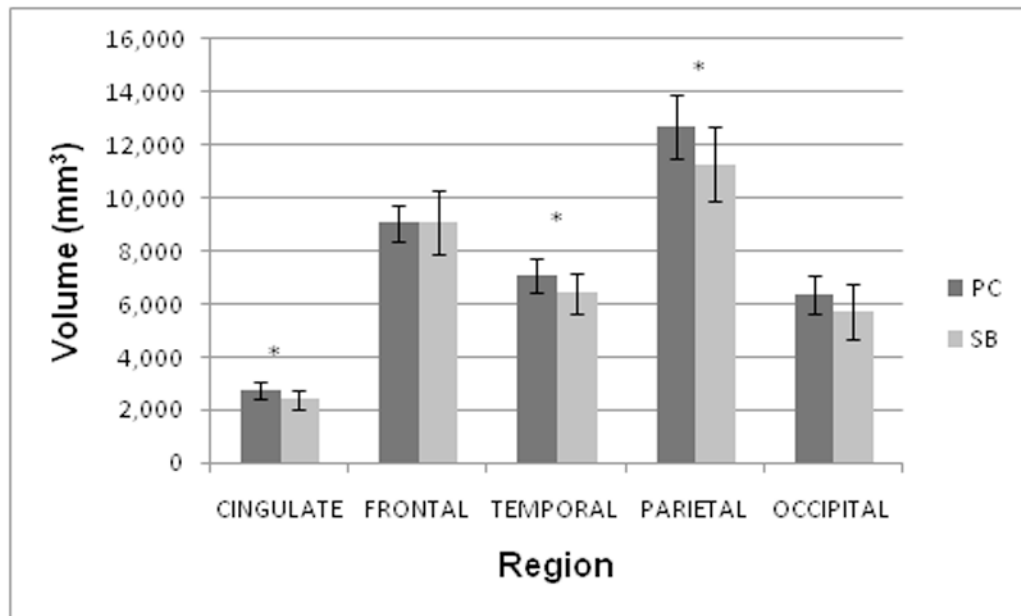


Figure 2. Average neocortical volume (mm³) for five ROIs in SB (n=16) and PC (n=16) groups
In all but the Frontal region, the trend is for the SB group to exhibit decreased volume relative to the PC group, reaching significance (*) in the Cingulate, Parietal, and Temporal regions.

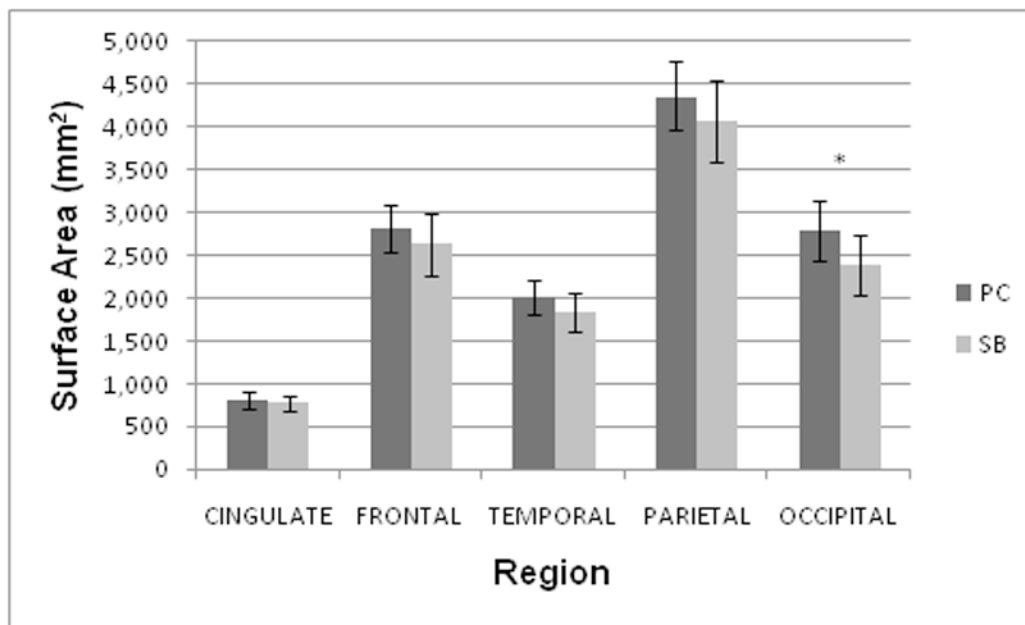


Figure 3. Average neocortical surface area (mm²) for five ROIs in SB (n=16) and PC (n=16) groups Significant main effect of Group (PC>SB). Significant interaction effects between group and ROI are limited to the Occipital Region (*).

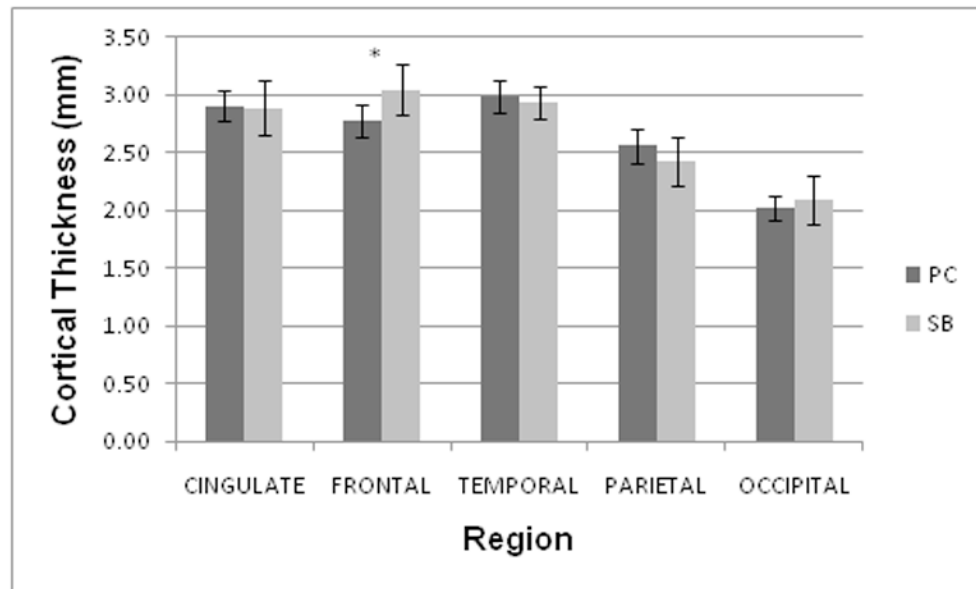


Figure 4. Average neocortical thickness (mm) for five ROIs in SB (n=16) and PC (n=16) groups. Significant interaction effects between Group and ROI are limited to the Frontal region where SB > PC (*).

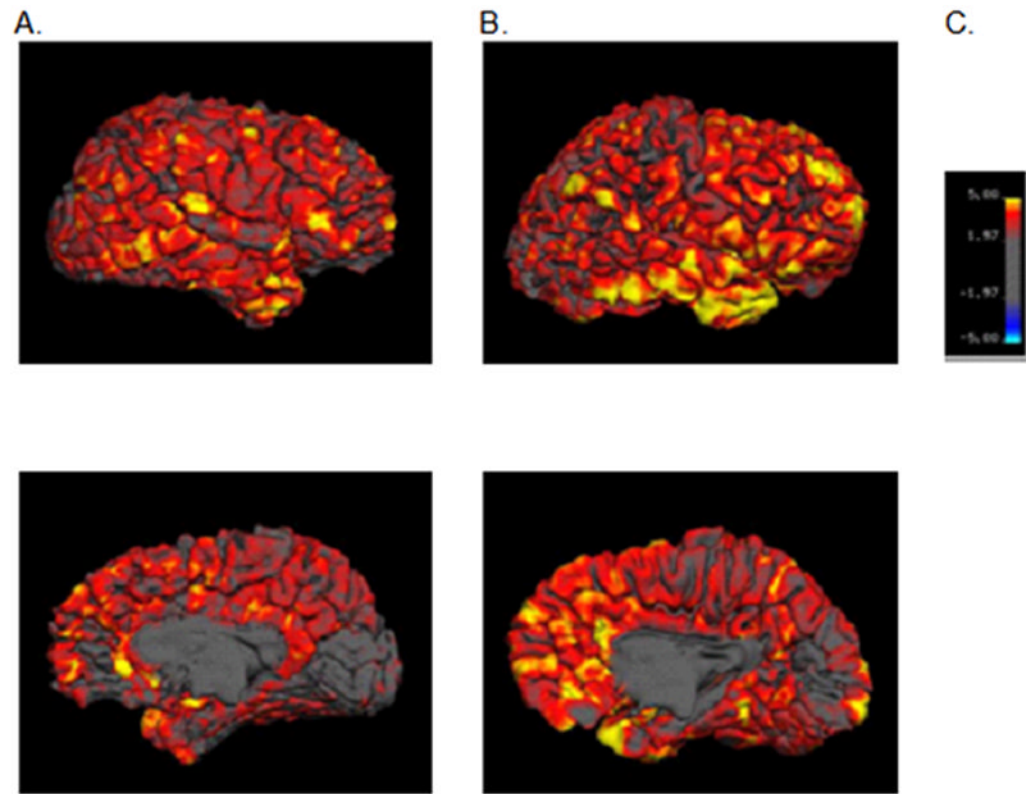


Figure 5. Example single subject surface maps of quantified cortical thickness shown on the right pial surface reconstructed from a PC (A) and an SB (B) subject
Color-coded scale bar (C) indicates cortical thickness values. Top row displays lateral surface. Bottom row displays medial surface.

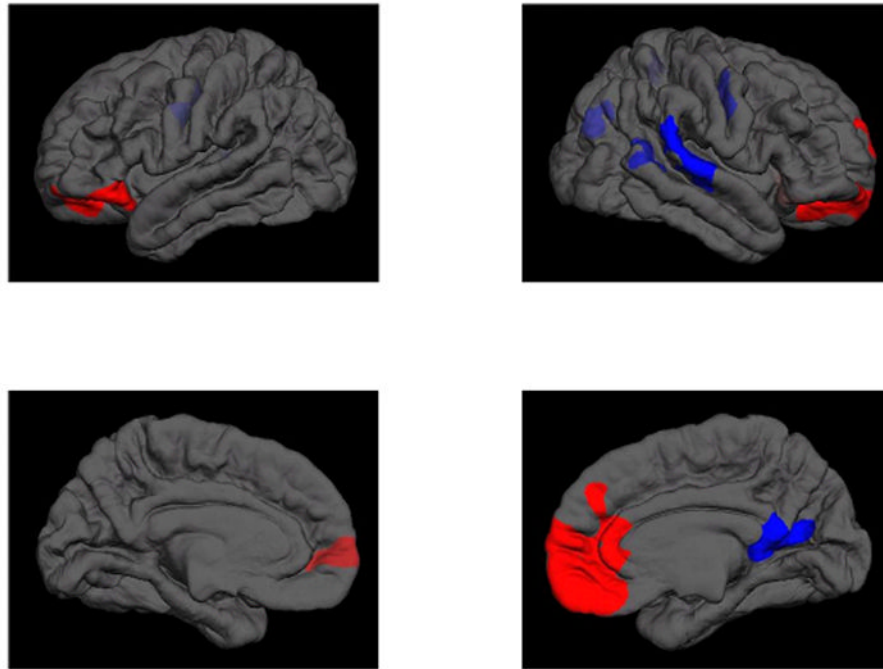
Left HemisphereRight Hemisphere

Figure 6. Significant group differences in average cortical thickness displayed on average pial surface of all subjects (n=32)
top row=lateral aspect; bottom row=medial aspect. Displayed clusters have been corrected for multiple comparisons: red clusters SB>PC ($p<0.001$); blue clusters indicate SB<PC ($p<0.001$).

Group Comparisons of Regional Volume (mm³), Surface Area (mm²), and Neocortical Thickness (mm). Values are presented as Mean (\pm SD).

Table 1

Region	Volume (mm ³)			Surface Area (mm ²)			Thickness (mm)			
	PC	SB	PC	SB	PC	SB	PC	SB	PC	
CINGULATE_LH	2734.61 (332.68)	2527.02(484.85)	813.47 (104.09)	795.75 (108.96)	2.91 (0.12)	2.91 (0.30)	2.91 (0.12)	2.91 (0.30)	2.91 (0.12)	2.91 (0.30)
CINGULATE_RH	2723.13 (424.09)	2240.45 (433.20)	807.22 (130.67)	743.63 (124.12)	2.90 (0.16)	2.87 (0.23)	2.90 (0.16)	2.87 (0.23)	2.90 (0.16)	2.87 (0.23)
CINGULATE_BI	2728.87 (325.19)	2383.74 (385.67)	810.34 (109.64)	769.69 (93.80)	2.91 (0.13)	2.89 (0.24)	2.91 (0.13)	2.89 (0.24)	2.91 (0.13)	2.89 (0.24)
FRONTAL_LH	8987.98 (706.55)	8943.47 (1084.59)	2790.93 (294.88)	2607.84 (328.14)	2.76 (0.14)	3.01 (0.23)	2.76 (0.14)	3.01 (0.23)	2.76 (0.14)	3.01 (0.23)
FRONTAL_RH	9143.84 (742.07)	9238.41 (1321.14)	2835.15 (289.63)	2657.53 (397.55)	2.79 (0.16)	3.07 (0.22)	2.79 (0.16)	3.07 (0.22)	2.79 (0.16)	3.07 (0.22)
FRONTAL_BI	9065.91 (701.61)	9090.94 (1189.98)	2813.04 (284.49)	2632.68 (359.33)	2.78 (0.15)	3.04 (0.22)	2.78 (0.15)	3.04 (0.22)	2.78 (0.15)	3.04 (0.22)
TEMPORAL_LH	7058.20 (644.06)	6552.97 (739.84)	1999.65 (205.02)	1858.04 (230.08)	2.99 (0.15)	2.97 (0.20)	2.99 (0.15)	2.97 (0.20)	2.99 (0.15)	2.97 (0.20)
TEMPORAL_RH	7107.81 (653.63)	6238.84 (759.41)	2028.58 (207.52)	1823.77 (234.37)	2.98 (0.15)	2.91 (0.11)	2.98 (0.15)	2.91 (0.11)	2.98 (0.15)	2.91 (0.11)
TEMPORAL_BI	7083.01 (629.03)	6395.90 (725.39)	2014.11 (202.21)	1840.91 (225.04)	2.99 (0.14)	2.94 (0.14)	2.99 (0.14)	2.94 (0.14)	2.99 (0.14)	2.94 (0.14)
PARIETAL_LH	12641.05 (1159.10)	11347.45 (1428.72)	4293.21 (365.12)	4072.09 (476.60)	2.59 (0.15)	2.46 (0.21)	2.59 (0.15)	2.46 (0.21)	2.59 (0.15)	2.46 (0.21)
PARIETAL_RH	12734.81 (1277.45)	11222.16 (1449.40)	4423.56 (452.52)	4061.24 (492.63)	2.53 (0.16)	2.40 (0.22)	2.53 (0.16)	2.40 (0.22)	2.53 (0.16)	2.40 (0.22)
PARIETAL_BI	12687.93 (1192.84)	11284.81 (1400.68)	4358.39 (403.48)	4066.66 (469.64)	2.56 (0.15)	2.43 (0.21)	2.56 (0.15)	2.43 (0.21)	2.56 (0.15)	2.43 (0.21)
OCCIPITAL_LH	6560.20 (861.78)	5792.95 (1283.20)	2873.02 (379.20)	2474.11 (394.64)	2.02 (0.12)	2.06 (0.22)	2.02 (0.12)	2.06 (0.22)	2.02 (0.12)	2.06 (0.22)
OCCIPITAL_RH	6169.66 (687.97)	5633.31 (955.15)	2710.48 (326.90)	2305.91 (340.63)	2.03 (0.10)	2.12 (0.22)	2.03 (0.10)	2.12 (0.22)	2.03 (0.10)	2.12 (0.22)
OCCIPITAL_BI	6364.93 (734.38)	5713.13 (1048.37)	2791.75 (343.40)	2390.01 (341.41)	2.03 (0.11)	2.09 (0.21)	2.03 (0.11)	2.09 (0.21)	2.03 (0.11)	2.09 (0.21)